Geofísica Internacional (2005), Vol. 44, Num. 3, pp. 221-230

A palaeomagnetic study of Upper Pliocene volcanic rocks in the area of the Levant Fault near Homs, western Syria

J. M. Abou-Deeb[1] and D. H. Tarling[2]

[1] *Department of Geology, The University of Damascus, Syria*

[2] *School of Earth Ocean & Environmental Sciences, University of Plymouth, U.K.*

Received: January 13, 2004; accepted: March 29, 2005

RESUMEN

La desmagnetización térmica de 75 sitios en rocas basálticas, la mayor parte a menos de 5 km de la Falla Levante, identifica direcciones de remanencia consistentes en la mayoría de los sitios. Las polaridades identificadas son Normales, Inversas e Intermedias, dominando las Inversas. Los sitios Normales e Inversos están magnetizados similarmente, 5.6±5.3 A/m, en tanto que los sitios Intermedios o direcciones indefinidas están algo más fuertemente magnetizados, 11.9±9.5 A/m. Las susceptibilidades de campo bajo son consistentes, 30.9±15.2 mSI, lo que implica que el campo geomagnético pudo haber sido algo más intenso que durante las polaridades Normales o Inversas. Cuando la media de las direcciones de los sitios Normales se invierten, todos los sitios tienen valores similares de la inclinación media, 48.2° (δInc. = 2.7°), pero la declinación media de las de los sitios muestra un patrón regional. Sitios de 3 regiones al oeste de la zona de Falla Levant (Marmarita, Qalat El-Hossen, Tel Kalakh) tienen declinaciones similares, 186° (δDec. = 5.4°), declinaciones que son consistentes con las esperadas para esta parte de Arabia para este tiempo. Sin embargo, todos los sitios al este y cercanos a la zona de Falla Levant (Bahur, W. Ain-Kut, Mzeineh y Buqeia) tienen declinaciones más al este, en promedio de 154.0±12.0°. La diferencia de declinación, 37.3°, indica la presencia de bloques rotados adyacentes al lado oriental de la Falla Levante. Tal rotación es consistente con el desplazamiento de 25 km predicho para esta localidad y parece consistente con la subsecuente evolución volcánica y tectónica de la Falla Levante, sugiriendo rotaciones significativas y actividad sísmica durante los últimos 5 Ma.

PALABRAS CLAVE: Paleomagnetismo, rotaciones tectónicas, Falla Levante, Plioceno superior, Siria, Líbano.

ABSTRACT

Thermal demagnetisation of samples from 75 sites in basaltic rocks, mostly within 5 km of the Levant Fault, identifies consistent directions of remanence in most sites. Normal, Reversed and Intermediate polarities are identified, with Reversed polarities dominating. The Normal and Reversed sites are similarly magnetised, 5.6±5.3 A/m, while those of sites of Intermediate or undefined direction are somewhat more strongly magnetised, 11.9±9.5 A/m. The low field susceptibilities are consistent, 30.9±15.2 mSI, implying the geomagnetic field may have been somewhat stronger than during Normal or Reversed polarity. When the mean directions of the Normal sites are reversed, all sites have similar mean inclination values, 48.2° (δInc. = 2.7°), but the site mean declinations show a regional pattern. Sites from the 3 regions west of the Levant Fault zone (Marmarita, Qalat El-Hossen, Tel Kalakh) have similar declinations, 186° (δDec. = 5.4°). These are consistent with those from the Sufer and E. Ain Kut regions, 197° (δDec. = 3.9°), furthest east of the Levant Fault zone. All these localities have directions that are consistent with those expected for this part of Arabia for this time. However, all sites east and close to the Levant Fault zone (Bahur, W. Ain-Kut, Mzeineh and Buqeia) have more eastern declinations, averaging 154.0±12.0°. The declination difference, 37.3°, indicates the presence of rotated blocks adjacent to the eastern side of the Levant Fault. Such a rotation is consistent with the 25 km displacement predicted for this location and appears consistent with the subsequent volcanological and tectonic evolution of the Levant Fault, suggesting significant rotation and seismic activity during the last 5 Ma.

KEY WORDS: Palaeomagnetism, tectonic rotations, Levant Fault, Upper Pliocene, Syria, Lebanon.

INTRODUCTION AND REGIONAL GEOLOGY

Syria occupies the northwestern part of the Arabian plate. The Coastal Mountain Range, in the northwestern part of the country, borders the northern end of the Levant transform fault system (Ponikarov, 1966; Best *et al*., 1993) - the northern-most extension of the Dead Sea transform fault system (Dubertret, 1970, Girdler, 1990). This fault enters Syria from northern Lebanon, where it is called the Yammouneh Fault, and, in Syria, forms the Missiaf Ghab fault system that widens in the north to form the rhomb-shaped Missiaf-Ghab graben (Sigachev *et al*., 1995). The Coastal Mountain Range occupies the western margin of this fault complex and has a largely monoclinal structure of mainly Jurassic and Cretaceous sedimentary rocks dipping towards the Mediterranean. The eastern margin of the fault complex consists of

Upper Cretaceous to Quaternary sedimentary and volcanic rocks. The Yammouneh and Missiaf-Ghab fault systems are together widely regarded as the major seismic zone in the area with a predicted left lateral displacement of about 20-25 km (Quennell, 1984; Trifonov *et al*., 1991). However, following detailed studies in the Lebanon, Butler *et al.* (1997) concluded that neither of these zones had been active during the past 5 Ma but that, during this time, seismic activity had mostly been associated with the Roum Fault that extends from south Lebanon through Beirut. As part of a regional study of late Tertiary volcanic rocks in NW Syria (Abou-Deeb *et al*., 1999), late Pliocene sites have been sampled on both sides of the Missiaf-Ghab fault system.

Following volcanic activity in the Mesozoic (Dubertret, 1933), there was a brief phase of volcanic activity in the Aleppo region during the Palaeogene (Mouty *et al*., 1992), followed by subaerial flood basalts in the Early Miocene, mostly 20 to 16 Ma ago. This extended over most of southern Syria, Jordan and Saudi Arabia, but was absent along the Syrian coastal zone (Mouty *et al*., 1992). A period of quiescence followed until c.8 My ago when intensive volcanism commenced over most of Syria, but particularly along the rift margins in the south and the Levant transform fault margins in the north (Figure 1). This phase of volcanism remained active into prehistoric time, for example, in the Karasu Valley in the northernmost part of the rift (Capan *et al*., 1987) where ages range from 2 My to 0.4 My. Studies of the mid Miocene volcanic sequences to the south-west of the Missiaf-Ghab fault system showed polarity differences that could be related to the oceanic magnetic anomaly sequences of the same age but no clear evidence of tectonic post mid-Miocene rotations in that area (Abou Deeb *et al*., 1999). This paper reports the results for 75 separate sites, each comprising 6-7 samples, in Upper Pliocene (map unit βN^{b}_{2}) basaltic flows, one certain dyke (T70-72) and two possible dykes (T61-63 and T46-48) mostly in highly faulted areas within some 5 km of the Levant Fault (Figure 1 and

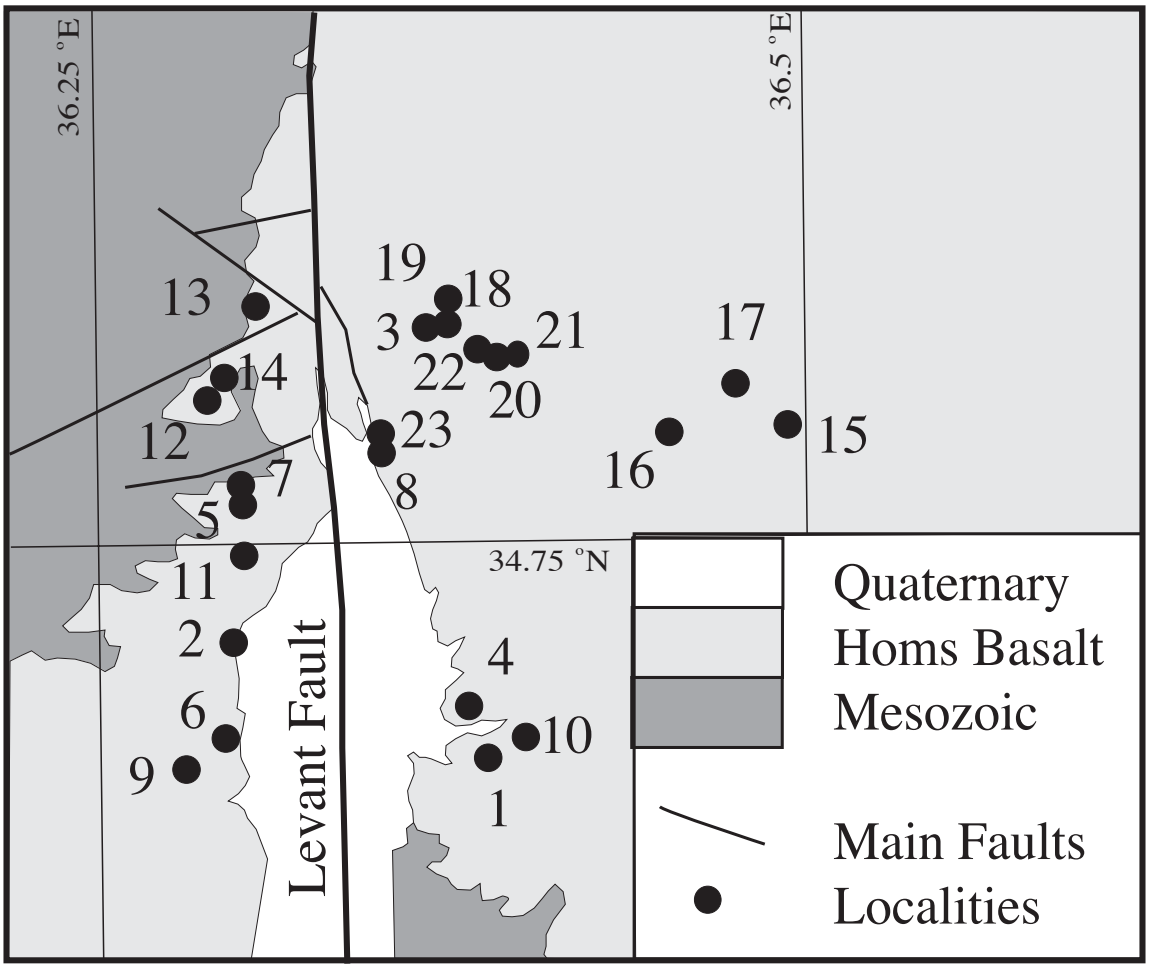

Fig. 1. Outline geological map of the studied area. The sampling localities represent mostly 3 sites per volcanic unit. The main N/S Levant fault is labelled, but, for clarity, the orientations of only a few relevant faults are marked. The Quaternary sequences are mostly unconsolidated sediments, dominated by those of the Al Bugeia Depression. The fault trends were mainly N-S, NW-SE and NE-SW directions but only the main faults systems can be shown.

Appendix). Generally, three sites were taken at separate locations, wherever possible in identical flows or, where the outcrop could not be physically traced between exposures, a flow at the equivalent elevation and with the same field characteristics and relationships.

SAMPLING, MEASUREMENT AND TREATMENT

Conventional palaeomagnetic drilling techniques (Collinson, 1983; Tarling, 1983) were employed and virtually all orientations were made using both sun and magnetic compasses. The field cores were sliced to provide standard samples, 2.5 cm in diameter and 2.1 cm in height. The intensity and direction of remanence was measured with a Digico spinner magnetometer (Molyneux, 1971) that has a background noise-level of *c*. 0.02 mA/m. Even excluding the exceptionally strongly magnetized T56 site (intensity 116.5 A/m), the initial intensity of magnetization was generally high, arithmetically averaging 7.05±6.86 A/m per site, and even the most weakly magnetic site, T66, had an average intensity of 0.59 A/m, well in excess of the instrumental noise level. The average site low-field susceptibilities ranged from 3.4 to 71.1 mSI. The anisotropy of magnetic susceptibility (AMS) of all samples was then measured before they were demagnetised at five temperature levels, 200, 250, 300, 350, 400°C, with representative samples from each of the main localities being treated at 100, 150, 200, 250, 300, 350, 400, 450, 500, 520, 540, 560 and 580°C. Sample characteristic directions were defined where the vectors isolated had a mean angular deviation (*MAD*) of ≤5° (Kirschvink, 1980). A site mean direction was considered further if it was defined by at least 5 samples with characteristic directions that agreed with an estimated 95% Probability cone of confidence of <15° (Fisher, 1953). Alternating magnetic field demagnetization up to 100 mT was also undertaken on samples from the same representative sites, but no reliable vectors could be isolated in any of these samples using this technique.

RESULTS AND INTERPRETATIONS

In the majority of sites, the samples had well defined characteristic directions during thermal demagnetisation, with their mean angular deviations (*MAD*) mostly being less than 3°. The main exceptions were in 5 sites (T4, T8, T13, T15, T59) in which most sample *MAD's* exceeded 5°; these sites were excluded from further directional analyses. In the remaining sites, the blocking temperature spectra suggested that the characteristic magnetic directions were carried by magnetite. Above about 350°C, the low field susceptibility tended to increase, but with no apparent effect on the linearity of the vector until approaching the Curie point of magnetite. In almost all samples, the temperature range within which a single vector was defined extended from 150-200° to at least 400°C (Figure 2). A well defined site mean direction was isolated in most remaining sites, with the site mean precision estimate, α_{95} (Fisher, 1953), being <15° (Table 1). However, 2 sites were rejected (T40 and T58) in which α_{95} >15° and a further 2 sites (T9 and T10) in which the number of acceptable sample directions became <5.

As expected for the Late Pliocene, both Normal (N) and Reversed (R) polarities were present. Using the standard definitions (N = site virtual geomagnetic pole [VGP] latitude >50°N; Reversed VGP >50°S; Intermediate = site VGP between 50°N and 50°S), the majority of the sites, 41, were of Reversed polarity, 12 were of Normal polarity and 16 were of Intermediate polarity. The arithmetic mean site initial intensity of magnetisation of the Reversed polarity sites (5.18±3.9 A/m) was similar to that of the 12 Normally magnetised sites (6.74 ±8.4 A/m). The 16 sites of Intermediate polarity sites were more strongly magnetised and much more scattered (18.4±27.7 A/m) and still remained more strongly magnetic (11.9 ± 9.5 A/m), but of similar scatter after removal of the most strongly magnetised site (T56). The 6 sites with scattered sample directions were also marginally more strongly magnetised (8.4±7.4 A/m) than those of Normal or Reversed polarity although their scatter became similar. In contrast, the low-field susceptibility site arithmetic mean values were similar, irrespective of polarity: Reversed (29.5 ± 17.3 mSI), Normal (34.4 ± 12.1 mSI), Intermediate (31.1 ± 13.1 mSI) and Scattered (32.3 ± 12.5 mSI). Both the initial intensity and low-field susceptibility values showed within-site variations that were an order of magnitude less than the between site variations. The distributions and ratios of these scalar values therefore suggests that the variations in the initial remanence are not likely to be due to the geomagnetic field may have been stronger during times of Intermediate polarity than of Normal or Reversed polarity. Such observations are also consistent with the observed remanences not having been affected by lightning, as also indicated by the consistency of the within and between site directions of remanence. The failure to isolate consistent components during alternating field treatment is therefore considered to be due to strong magnetic viscosities, possibly implying large ferromagnetic grain-sizes. Lightning is not indicated by the high within-site consistency of sample directions or by the rate of decrease in intensity, averaging only 50% by 200°C. The magnitude of anisotropy (P_J - Jelinek, 1981) being mostly between 1.01 and 1.04 in the lavas. The fabric is oblate in two thirds of the samples, the rest being prolate with few neutral fabrics. Such parameters are typical for non-tectonised lavas and there are no distinguishable differences between the AMS parameters in any of the localities. The magnetic anisotropy, currently being incorporated with local structural analyses, is therefore unlikely to have affected the observed directions in any consistent manner.

For tectonic interpretations, it is desirable to reduce any geomagnetic secular variation or non axial dipole effects from the observed directions of remanence. On this basis, all 16

Table 1

Site Mean Intensity, Susceptibility and Direction of Remanence

Site	N/n	Init. Int. (A/m)	Susc. (mSI)	Direction Decl.	Incl.	*k*	α_{95}	Virtual Pole Lat.	Long	Pol
Western flank										
Marmarita										
T40	5/6	7.4±1.1	36.6±2.3	scattered		21	17.0	scattered		S
T41	5/6	5.3±0.2	8.6±1.9	112.7	-62.2	1671	1.9	-38.5	157.5	I
T42	6/6	2.2±0.8	6.8±1.1	170.5	-66.9	134	5.8	-73.7	193.8	R
T43	6/6	21.5±3.3	30.9±1.5	73.9	4.3	161	5.3	14.4	133.9	I
T44	6/6	31.4±4.9	28.1±1.0	57.4	5.4	423	3.3	28.0	144.0	I
T45	6/6	12.2±1.47	21.9±3.6	33.4	16.3	300	3.9	49.6	159.3	I
T46pd	5/6	1.86±0.45	63.4±2.1	175.8	-54.1	165	6.0	-86.5	125.2	R
T47pd	5/6	2.27±0.26	49.7±1.5	182.5	-43.1	318	4.3	-80.0	22.9	R
T48pd	6/6	1.87±0.17	53.6±2.2	185.4	-42.4	483	3.1	-78.7	10.5	R
Qalat El-Hossen										
T19	6/6	5.2±0.3	21.2±1.7	195.5	-49.2	944	2.2	-76.2	321.9	R
T20	5/6	3.0±0.1	6.8±0.7	189.9	-49.9	1319	2.1	-80.8	329.9	R
T21	6/6	3.1±0.1	10.6±2.0	187.7	-48.1	1375	1.8	-81.4	344.8	R
T25	4/7	4.7±1.4	38.0±3.5	132.1	-18.3	43	14.2	-39.5	107.9	I
T26	6/6	4.4±0.6	44.1±3.0	131.0	-13.2	308	3.8	-37.0	106.1	I
T27	6/6	2.9±0.9	32.1±1.3	145.0	-24.1	178	5	-51.4	100.0	R
T37	6/7	8.4±1.6	20.0±6.2	192.8	-32.5	162	4.8	-69.4	359.3	R
T38	5/6	12.4±1.8	22.5±2.4	209.0	-7.7	54	10.5	-49.1	348.7	R
T39	6/6	11.3±1.9	22.7±2.0	195.6	-21.2	240	4.5	-62.3	1.6	R
Tel Kalakh		8.5±0.8 Ma[2]								
T4		2.8±0.5	32.4±1.0	undefined						S
T5	5/6	5.4±1.9	31.9±6.7	120.3	-59.9	121	7.0	-43.3	152.3	I
T6	4/6	3.4±1.4	11.3±5.1	109.6	-56.1	175	7.0	-34.1	150.4	I
T7	5/6	4.2±0.7	13.4±2.6	115.6	-54.7	231	5.0	-38.2	146.6	I
T8		4.5±0.4	7.9±0.4	undefined					S	
T22	6/6	2.7±0.4	71.1±3.0	175.8	-48.6	467	3.1	-83.7	72.2	R
T23	6/6	4.0±1.5	57.2±11.0	177.5	-51.4	1057	2.1	-86.6	75.8	R
T24	6/6	5.9±1.0	65.4±4.4	173.7	-49.6	1091	2.0	-83.2	89.6	R
T31	6/6	3.8±0.3	30.2±2.2	190.9	-51.2	77	7.7	-80.4	320.4	R
T32	7/7	3.9±1.0	33.5±1.8	197.5	-47.5	347	3.2	-73.9	323.6	R
T33	7/7	5.5±1.2	31.7±0.8	198.2	-49.6	45	9.1	-74.1	316.8	R
Eastern Flank										
E. Ain-Kut		5.25±0.2; 5.08±0.16 Ma[1]								
T64	6/6	1.7±0.4	13.9±5.0	199.4	-43.1	1915	1.5	-70.6	331.3	R
T65	6/6	1.0±0.1	6.2±0.4	199.0	-45.9	1760	1.6	-72.1	325.9	R
T66	6/6	0.6±0.1	3.4±0.3	194.2	-50.2	727	2.5	-77.5	320.4	R
T67	5/6	1.6±0.3	27.2±3.6	199.4	-51.6	574	3.2	-73.7	309.9	R
T68	6/6	1.6±0.2	24.9±5.0	202.4	-40.8	108	6.5	-67.4	330.8	R
T69	6/6	2.5±0.7	40.3±2.3	199.7	-44.9	440	3.2	-71.2	327.2	R
W. Ain-Kut										
T70[d]	6/6	7.1±0.6	6.1±0.9	165.9	-47.8	1667	1.6	-76.6	103.7	R

T71[d]	6/6	8.5±1.1	10.6±1.0	163.0	-47.9	1556	1.7	-74.5	109.1	R
T72[d]	6/6	20.9±3.4	7.6±2.2	171.5	-41.3	1581	1.7	-76.7	72.4	R
Bahur		6.2±0.2 Ma; 5.21±0.17 Ma; 5.08±0.16 Ma[1]								
T9	3/6	1.7±0.2	11.7±1.5	(175.4	-19.0)	124	11.1	-64.6	47.0	R
T10	3/6	3.0±0.4	30.5±1.6	(156.82	-25.9)	207	8.6	-60.2	86.8	R
T11	5/6	4.0±1.0	31.1±3.1	146.7	-40.5	136	6.6	-58.8	113.4	R
T12	5/6	3.5±0.6	25.7±2.9	164.3	-46.7	86	8.3	-75.0	103.4	R
T58	4/6	22.9±18.1	43.3±2.3		highly scattered					S
T59	2/6	26.2±10.2	33.6±2.4	(294.0	-57.3)	575	10.4	(-5.0	262.7)	I
T60	4/6	3.9±0.2	34.3±1.0	19.6	56.8	195	6.6	74.0	111.6	N
T61[pd]	6/6	3.9±0.2	38.7±1.2	343.2	53.7	163	5.3	76.1	308.8	N
T62[pd]	6/6	3.6±0.2	57.5±3.1	338.2	55.3	380	3.4	72.2	316.1	N
T63[pd]	6/6	2.9±0.2	36.8±2.4	347.6	45.8	321	3.7	76.9	274.1	N
Mzeineh										
T28	4/6	4.4±2.4	17.0±2.5	0.4	48.4	127	8.2	84.6	212.6	N
T29	5/6	2.4±0.5	15.6±2.3	143.2	-37.8	158	6.1	-55.1	113.3	R
T30	6/6	3.1±0.2	18.4±3.0	128.4	-27.3	161	5.3	-39.5	116.1	I
T73	6/6	7.3±0.7	24.7±1.8	342.1	51.3	153	5.4	74.8	300.8	N
T74	4/6	5.4±0.4	27.9±1.5	342.7	72.0	40	14.7	65.0	13.8	N
T75	6/6	33.0±1.3	14.8±0.7	314.7	51.6	519	2.9	52.4	315.7	N
Sufer		4.85±0.15 Ma; 5.64±0.18[1]								
T49	6/6	3.9±0.4	33.5±2.0	18.1	46.9	618	2.7	73.2	144.9	N
T50	6/6	3.8±0.4	40.6±2.9	12.2	45.8	379	3.4	77.1	159.3	N
T51	6/6	3.1±0.3	47.9±1.8	12.2	46.5	643	2.6	77.5	157.3	N
T52	6/6	11.9±3.8	48.4±1.8	314.7	-1.7	659	2.6	34.7	276.3	I
T53	6/6	19.6±3.2	51.0±6.2	308.8	0.2	452	3.2	31.0	281.9	I
T54	5/6	20.2±1.0	39.8±1.7	254.7	-1.2	1126	2.3	-12.9	314.9	I
T55	6/6	5.0±1.7	40.7±4.0	256.1	-8.0	112	6..4	-13.7	311.1	I
T56	6/6	116.5±5.1	37.4±2.5	257.5	-17.5	325	3.7	-15.3	306.1	I
T57	5/6	5.8±2.0	38.9±6.7	17.8	52.4	122	6.9	75.1	128.3	N
Buqeia		5.4±0.1 Ma[2]								
T1	7/7	7.0±0.9	40.1±2.5	144.8	-48.9	166	4.7	-60.0	127.1	R
T2	5/6	5.2±0.6	43.1±3.3	141.9	-43.9	139	6.5	-56.1	121.6	R
T3	6/6	6.3±1.0	40.8±2.6	151.3	-48.9	225	4.5	-65.3	123.0	R
T13		8.6±1.3	34.8±2.4		undefined				S	
T14	5/6	9.3±3.7	33.2±1.3	145.1	-46.9	164	7.2	-59.6	123.6	R
T15		4.1±0.7	38.8±1.0		undefined				S	
T16	6/6	4.5±2.8	30.9±0.7	167.7	-50.0	179	5.0	-78.9	109.2	R
T17	6/6	5.65±0.4	41.1±2.2	166.5	-44.8	241	4.3	-75.7	94.5	R
T18	6/6	9.5±0.5	36.0±1.3	147.4	-22.6	296	3.9	-52.5	96.6	R
T34	6/6	7. 6±0.8	29.5±1.5	136.1	-45.9	709	2.5	-52.0	127.6	R
T35	6/7	6.5±3.6	41.2±4.0	151.4	-48.9	701	2.5	-65.4	123.0	R
T36	6/6	10.9±4.3	22.4±1.8	134.5	-40.8	87	7.2	-49.0	122.9	R

All sites are extrusive rocks, with the exception of T70-72, marked [d] and T61-62 and T44-48 that are probably dykes, marked [pd]. Radiometric date references are [1] Novikov *et al.* (1993) and [2] Mouty *et al.* (1992). The number of samples per site, with a vector defined with a mean angular deviation (*MAD*) less than 5° (Kirshvink, 1980), is N compared with the total number of samples collected, n. The mean initial intensity of magnetisation (Init. Int.) is in units of A/m and the mean susceptibility are in mSI units. The means and standard deviations of the intensity and susceptibility assume a normal Gaussian distribution. The site mean directions (Declination, Decl. and Inclination, Incl.) are listed with the estimates of precision , *k*, and 95% Probability, α_{95} (Fisher, 1953). The polarity (Pol.) of each site is Normal (N), when the virtual geomagnetic pole latitude is greater than 50°N, Reversed (R), when greater than 50°S, and Intermediate (I) when between these two limits. "Scattered" sites (S) are when there are fewer than 5 samples with *MAD* < 5° or when the site precision, α_{95}, exceeds 15°.

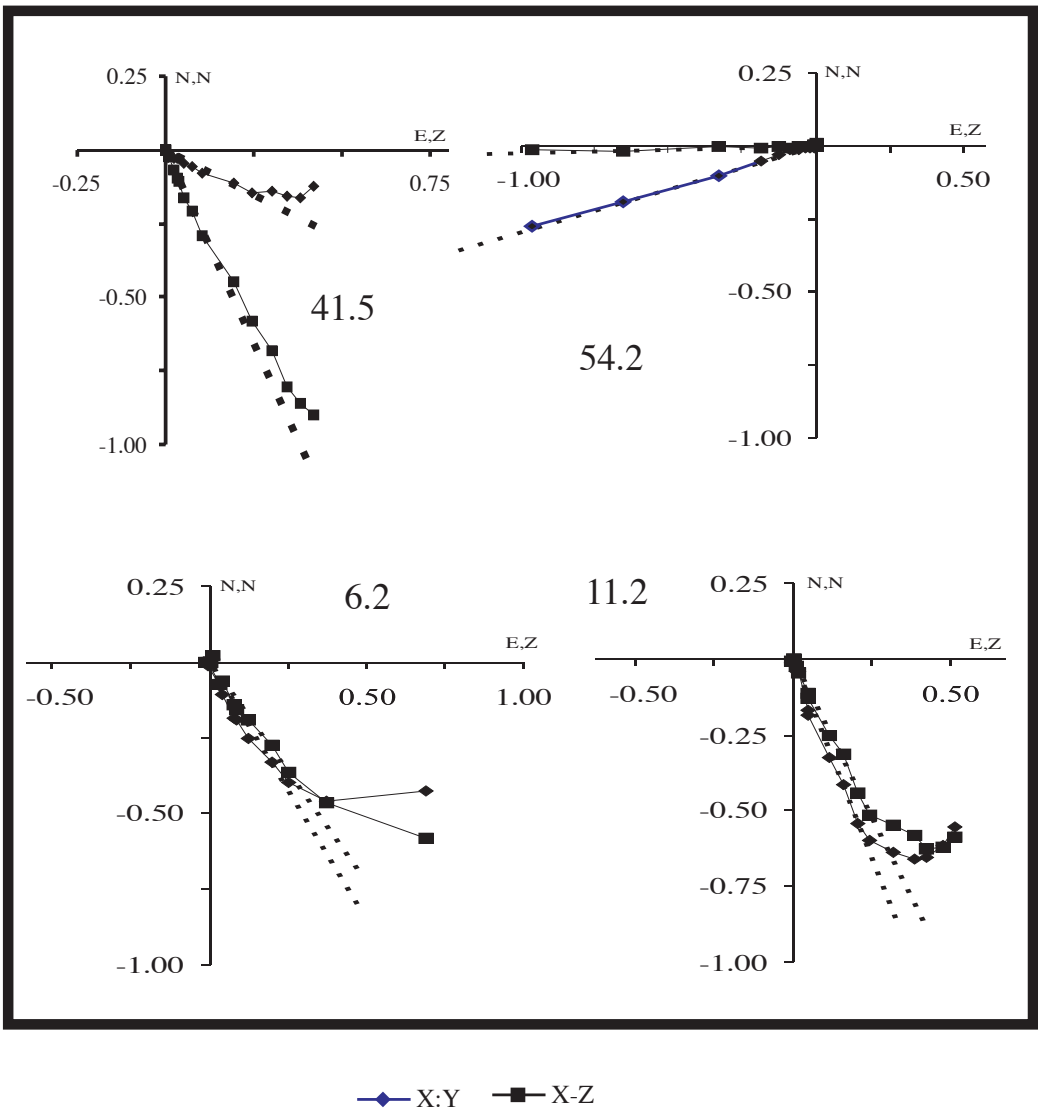

Fig. 2. Examples of thermal demagnetisation behaviour. These Zijderveld plots illustrate the vector changes during incremental heating (100°, 150° 200°, 250°, 300°, 350°, 400°, 450°, 500°, 520°, 540°, 560° and 580°C) in zero external magnetic field. The components shown are declination (diamond; x *vs*. y) and vertical (square; x *vs*. z) with the normalised intensity (the ratio to the initial value - given below). The best-fitting line, constrained to pass through the origin, and excluding secondary components and weak values at high temperatures, is shown dashed. The top two examples are from stable regions; T41.5 from Marmarita in the West (initial intensity 5.61 Am and Reversed polarity), and T54.2 from Sufer in the East of Intermediate polarity (20.4 Am). The lower two are from rotated regions and both of Reversed polarity; T02.6 from Buqeia in the south (5.91 Am) and T11.2 from Bahur in the north (4.44 Am).

sites of Intermediate polarity were ignored and the polarity of the Normal sites were reversed by 180° so that all remaining 53 mean site vectors were southerly and of negative inclination (191.3°, 48.2°, α_{95}=2.7°). However, of these sites, there were some that were more divergent from the overall mean direction than others, particularly in inclination. Assuming that tectonic rotations related to a major transcurrent fault system would be largely about vertical axes, 11 site mean directions were initially rejected as having inclinations more than 8° (solid angle) from the overall mean inclination. The remaining 42 sites showed two clear declination populations – one SSW (between 182-195°) and the other SSE (between 146-167°). When plotted (Figure 3) these populations showed a distinct regional distribution. All SSW declinations are confined to the three regions west of the main Levant Fault (Marmarita, Qalat El-Hossen and Tel Kalakh 185.9°, -49.0°, α_{95}=3.6°) and the two regions more than *c*. 5 km east of the Fault (E. Ain-Kut and Sufer 197.5°, -46.8°, α_{95}=2.6°). These had a combined mean direction of 191.3°, -48.2° (α_{95} = 2.7°). Such a direction is consistent with that predicted for this part of Arabian some 10 Ma, 185.6°, -49.9°, i.e. after allowing for the opening of the Red Sea and using the African polar wander path (Besse and Courtillot, 1991). This implies that such regions belong to the stable part of the

Table 2

Regional Mean Directions

Locality	Sites	Decl.	Incl.	*k*	α_{95}	Site Numbers
Western Flank						
Marmarita	3	181.6	-46.6	122	11.2	T46-T48
Qalat El-Hossen	3	191.0	-49.1	843	4.3	T19-T21
Tel Kalakh	6	185.7	-50.1	119	6.2	T22-T24, T31-T33
Far Eastern Flank						
E. Ain-Kut	3	199.1	-46.1	321	3.7	T64-T69
Sufer	4	195.0	-47.9	464	4.3	T49-T51, T57
Near Eastern Flank						
W. Ain-Kut	3	167.0	-45.7	278	7.3	T70-T72
Bahur	5	159.7	-48.7	95	7.9	T11,T12, T61-T63
Mzeineh	3	146.4	-47.4	45	18.6	T29, T73, T75
Buqeia	9	148.5	-47.1	87	5.5	T1-T3, T14, T16, T17, T34-T36
Western Flank	12	185.9	-49.0	149	3.6	
Far Eastern Flank	10	197.5	-46.8	352	2.6	
"Stable" Zones	22	191.3	-48.2	138	2.7	
Rotated Zone	20	153.8	-47.6	71	3.9	

Abbreviations as for Table 1.

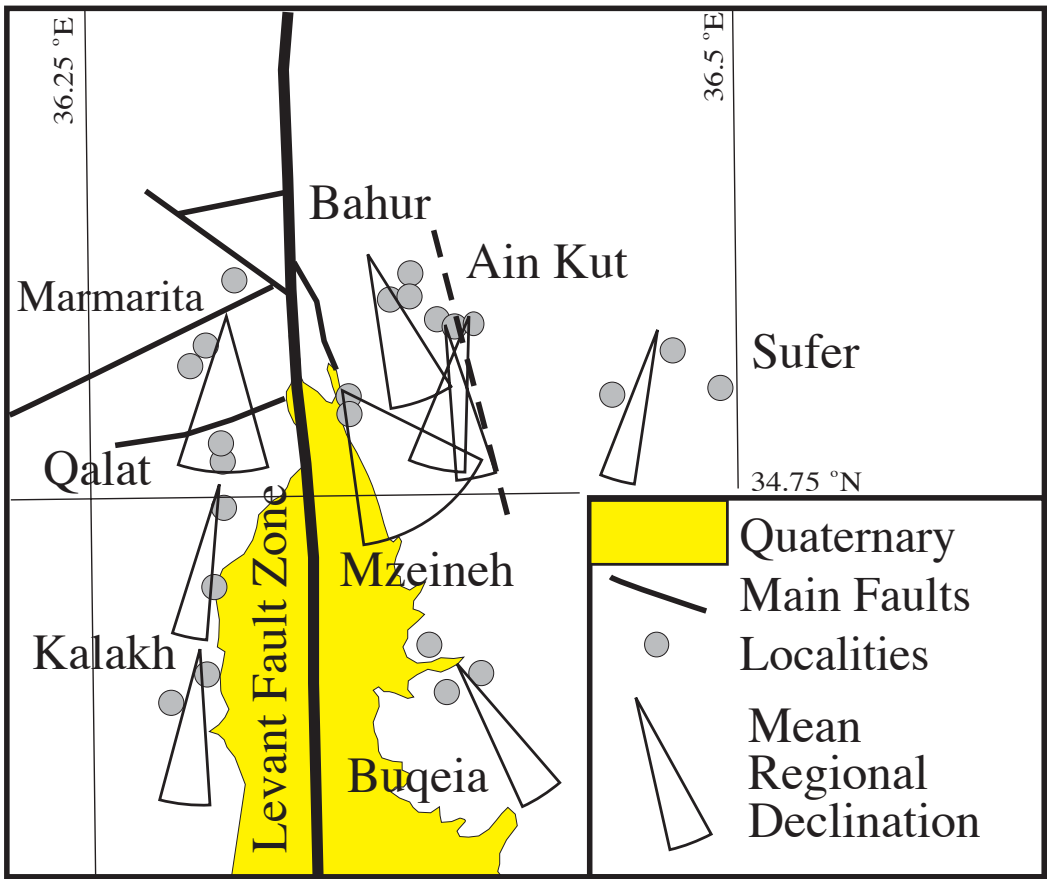

Fig. 3. The Pattern of Mean Regional Declinations. The circles, unlabelled, are the same locations as in Figure 1. The "pie wedges" are centred on the mean declination for each region, as listed in Table 2 and after inverting Normal polarities to Reversed, with the angle subtended by the wedge being based on error in declination, ±δDec., using the regional estimate of precision, α_{95}, given in Table 2.

Arabian Plate. In contrast, the sites in the eastern regions close to the Levant Fault (Bahur, W. Ain-Kut, Mzeineh and Buqeia) all have SSE site mean declinations, with a mean direction of 153.8°, -47.6° (α_{95} = 3.9°). This direction differs significantly in declination, by 37.7°, but is identical in inclination, suggesting that these sites are from areas that have been rotated anticlockwise, relative to stable Arabia, since they were formed some 5-6 Ma. (To avoid subjectivity, the 11 sites with mean inclinations >8° from the overall mean were re-included but did not alter the mean direction and only marginally decreased its precision.)

The western edge of this block is clearly the main Levant Fault itself, but the eastern flank is only defined in this study by the deep Al-Mnshar wadi, oriented N/S, that separates the sites in East and West Ain-Kut. It also suggests that the depressions, such as that of the Al Buqeia plain is a result of this rotation in a similar way to that of the Al Ghab Depression to the North. The apparent rotation of these eastern tectonic units within some 5 km of the main fault complex was not expected. It had originally been considered that far smaller units, possibly confined within the fault zone, may have defined the activity along this part of the Levant Fault. The scale of dislocation observed is consistent with the 20-25 km of differential motion predicted for this segment of the Dead Sea Fault system (Quennell, 1984; Trifonov *et al*., 1991), as is the anticlockwise sense of rotation that would be associated with a right-lateral displacement. The precise timing of the rotation, other than being post Homs Basalts (5-6 Ma), is uncertain. However, the continuation of volcanic activity in the region suggests that such motions may have been quasi-continuous during this period. The rotation would certainly be associated with contrasting areas of compression and tension – the tensional areas being likely sources for the intermittent intrusion and extrusion of volcanic materials that has continued into historical times. Such observations would suggest that seismic activity was also quasi continuous along this part of the Levant Fault from at least Upper Pliocene times until the present day.

ACKNOWLEDGEMENTS

We are particularly grateful to the University of Damascus for supporting the project, in particular the Dean of Science, Prof. Said Mahasneh, and the head of the Geology Department, Prof. Nassoh Khiami. The British Council is thanked for enabling the co operation necessitated by this work. The Department of Geology, University of Plymouth, is thanked for making facilities available for measurement and analysis as part of the concordat between the Universities of Plymouth and Damascus. We would particularly like to thank Dr. Tony Morris for his suggestions, and Dr. Samir Hanna of the Syrian General Establishment of Geology & Mineral Resources is thanked for his help in identifying the sample locations of Novikov *et al*. (1993).

APPENDIX

Site locations

Site	Latitude	Longitude	Location
T1	34 41 10	36 23 01	500 m E of Buqeia, RHS of Homs-Safita road
T2	34 41 10	36 23 01	20 m E of T1
T3	34 41 10	36 23 01	10 m E of T2
T4	34 43 07	36 17 51	end of Shmiseh village, 100 m to LHS of road
T5	34 43 07	36 17 51	10 m S of T4
T6	34 43 07	36 17 51	6 m S of T5
T7	34 43 07	36 17 51	5 m S of T6
T8	34 43 07	36 17 51	5 m S of T7
T9	34 48 43	36 22 03	500 m before Bahur village, LHS of road
T10	34 48 43	36 22 03	10 m S of T9
T11	34 48 43	36 22 03	6 m S of T10
T12	34 48 43	36 22 03	8 m S of T11
T13	34 42 00	36 23 00	2 km E of eastern Buqeia road
T14	34 42 00	36 23 00	4 m N of T13
T15	34 42 00	36 23 00	12 m N of T14
T16	34 42 00	36 23 00	5 m N of T15
T17	34 42 00	36 23 00	15 m N of T16
T18	34 42 00	36 23 00	20 m N of T17
T19	34 45 21	36 17 43	10 m SE of Qalat El-Hossen (Krack des Chevaliers)
T20	34 45 21	36 17 43	5 m S of T19
T21	34 45 21	36 17 43	5 m S of T20
T22	34 41 29	36 17 52	western end of Buqeia, hill on the RHS of road
T23	34 41 29	36 17 52	5 m W of T22
T24	34 41 29	36 17 52	10 m W of T23
T25	34 46 19	36 18 13	1 km from Qalat El-Hossen and Marmarita junction
T26	34 46 19	36 18 13	5 m N of T25
T27	34 46 19	36 18 13	6 m S of T25
T28	34 46 27	36 20 18	In the middle of Al-Mzeineh village
T29	34 46 27	36 20 18	3 m N of T28
T30	34 46 27	36 20 18	2 m S of T28
T31	34 41 01	36 16 44	500 m E of Tel-Kalakh Traffic Police Station
T32	34 41 01	36 16 44	5 m E of T31
T33	34 41 01	36 16 44	2 m higher than T32
T34	34 41 19	36 23 37	3 km E of Buqeia, RHS of Homs-Safita road
T35	34 41 19	36 23 37	25 m E of T34
T36	34 41 19	36 23 37	10 m W of T34
T37	34 44 50	36 18 08	Haart Al-Tourkman S of Qalat El-Hossen
T38	34 44 50	36 18 08	10 m N of T37
T39	34 44 50	36 18 08	3 m E of T38

Site	Latitude	Longitude	Location
T40	34 47 39	36 17 31	1 km on the mountain after Al-Nasra
T41	34 47 39	36 17 31	5 m S of T40
T42	34 47 39	36 17 31	10 m S of T41
T43	34 48 42	36 18 02	5 km after Al-Nasra, 150 m to RHS of road
T44	34 48 42	36 18 02	3 m E of T43
T45	34 48 42	36 18 02	4 m E of T44
T46	34 47 45	36 17 46	1.5 km on the mountain after Al-Nasra
T47	34 47 45	36 17 46	6 m E of T46
T48	34 47 45	36 17 46	6 m E of T47
T49	34 47 06	36 29 27	1.5 km east of Sufer village, over the bridge
T50	34 47 06	36 29 27	5 m south of T49
T51	34 47 06	36 29 27	5 m south of T50
T52	34 46 46	36 27 15	1 km west of Sufer village, LHS of road
T53	34 46 46	36 27 15	2 m before T52
T54	34 46 46	36 27 15	4 m before T53
T55	34 47 19	36 28 36	0.5 km north of Sufer village, in small hill
T56	34 47 19	36 28 36	5 m east of T55
T57	34 47 19	36 28 36	10 m east of T56
T58	34 48 42	36 22 18	0.8 km after Bahur, LHS of road
T59	34 48 42	36 22 18	10 m north of T58
T60	34 48 42	36 22 18	10 m south of T58
T61	34 48 56	36 22 29	inside Bahur, over the bridge
T62	34 48 56	36 22 29	10 m west of T61
T63	34 48 56	36 22 29	30 m east of the bridge
T64	34 48 04	36 2305	western end of Ain-Kut
T65	34 48 04	36 23 05	6 m north of T64
T66	34 48 04	36 23 05	6 m north of T65
T67	34 48 04	36 23 10	west of Ain-Kut, about 200 m south of T64-T66
T68	34 48 04	36 23 10	2 m east of T67
T69	34 48 04	36 23 10	20 m east of T68
T70	34 48 08	36 22 45	1.5 km west of Ain-Kut, in a dike crossing the road
T71	34 48 08	36 22 45	8 m south of T70
T72	34 48 08	36 22 45	10 m south ot T71
T73	34 46 49	36 20 09	north of Mzeineh, over the water canal
T74	34 46 49	36 20 09	2 m north of T73
T75	34 46 49	36 20 09	10 m north of T74

BIBLIOGRAPHY

ABOU-DEEB, J . M., M. M. OTAKI, D. H. TARLING and A. L. ABDELDAYEM, 1999. A palaeomagnetic study of Syrian volcanic rocks of Miocene to Recent age. *Geofis. Int., 38, (1)*, 17-26.

BESSE, J. and V. COURTILLOT, 1991. Revised and synthetic apparent polar wander paths of the African, Eurasian, North American and Indian Plates, and true polar wander since 200 Ma. *J. Geophys. Res., 96,* 4029-4050.

BEST, J., M. BARAZANGI, D. AL-SAAD, T. SAWAF and A. GEBRAN, 1993. Continental margin evolution of the northern Arabian platform in Syria. *Amer. Assoc. Petrol. Geol., Bull., 77,* 173-193.

BUTLER, R. W. H., S. SPENCER and H. M. GRIFFITH, 1997. Transcurrent fault activity on the Dead Sea Transform in Lebanon and its implications for plate tectonics and seismic hazard. *Jour. Geol. Soc., London, 154,* 757-760.

CAPAN, U. Z., PH. VIDAL and J. M. CANTAGREL, 1987. K-Ar, Nd, Sr and Pb isotopic study of Quaternary volcanism in Karasu valley (Hatay), N-end of the Dead Sea Rift zone in SE Turkey. *Yerbilimleri, 14,* 165-178.

COLLINSON, D. W., 1983. Methods and Techniques in Rock Magnetism and Palaeomagnetism, Chapman and Hall, London, pp.503.

DUBERTRET, L., 1933. Le Miocene en Syrie et au Liban, *Notes et Mémoires Syrie et Liban, 1,* 13-28.

DUBERTRET, L., 1970. Review of the structural geology of Red Sea and surrounding areas; Royal Society of London Philosophical Transaction, ser. A, 267, 9-20.

FISHER, R. A., 1953. Dispersion on a sphere. Proc. Roy. Soc., A217, 295-305.

GIRDLER, R. W., 1990. The Dead Sea transform fault system. *Tectonophysics, 180*, 1-13.

JELINEK, V., 1981. Characterization of the magnetic fabric of rocks. *Tectonophysics, 79,* 63-67.

KIRSCHVINK, J. L., 1980. The least-squares line and plane and the analysis of palaeomagnetic data. *Geophys. J. R. astr. Soc., 62*, 699-718.

MOLYNEUX, L. M., 1971. A complete results magnetometer for measuring the remnant magnetisation of rocks. G*eophys. J. R. astr. Soc., 24,* 429-433.

MOUTY, M., M. DELALOYE, D. FONTIGNIE, O. PISKIN and J. WAGNER, 1992. The volcanic activity in Syria and Lebanon between Jurassic and the Actual. *Schweiz. Mineral. Petrogr. Mitt., 72*, 91-105.

NOVIKOV, V. M., E. V. SHARKOV, I. V. CHERNYSHEV, E. V. DEVYATKIN, A. E. DODONOV, V. V. IVANENKO, M. I. KARPENKO, S. HANNA and N. HATUM, 1993. Geochronology of Weathering Crusts on Flood Basalts in Syria, and the Evolution of Regional Palaeoclimate during the last 20 Ma. *Stratigraphy and Geological Correlation, 1,* 627-635.

PONIKAROV, V. P., 1966. Editor Explanatory notes on the Geological Map of Syria: Homs Triboli Sheet, Scale 1:200,000, Ministry of Industry, Damascus, Syria.

QUENNELL, A. M., 1984. The Western Arabian rift system. *In:* Dixon, J.E. & Robertson, A.H.F. (eds) The Geological Evolution of the Eastern Mediterranean. Geological Society, London. Special Publication, 17, 775-788.

SIGACHEV, S. P, M. I. KOPP, K. ELIAS, A. HAFEZ, Z. H. ADZHAMYAN and F. FAKYANI, 1995. Tectonic data for the Levant fault by using mesotectonic measures (Ghab and Missiaf areas). *Geological Sciences Review, Damascus, 5,* 75-81, (In Arabic).

TARLING, D. H., 1983. Palaeomagnetism, Chapman & Hall, London, pp.379

TARLING, D. H. and F. HROUDA, 1993. The Magnetic Anisotropy of Rocks, Chapman and Hall, London, pp. 217.

TRIFONOV, V. G., V. M. TRUBIKHIN, Z. ADZHAMYAN, S. DZHALLAD, Y. EL-KHAIR and K. AYED, 1991. Levant fault zone in northwest Syria. *Geotectonics, 25,* 145-154.

J. M. Abou-Deeb[1] and D. H. Tarling[2,*]

[1] Department of Geology, The University of Damascus, Syria
[2] School Earth Ocean & Environmental Sciences, University of Plymouth, PL4 8AA, U.K.
[*] Corresponding author: Email: d.tarling@plymouth.ac.uk
Fax: +44(0)1752 2331117